Simulation of Sloshing Dynamics in a Tank by an Improved Volume-of-Fluid Method

Rik Wemmenhove[1], Bogdan Iwanowski[1], Marc Lefranc[1], Arthur E.P. Veldman[2], Roel Luppes[2], Tim Bunnik[3]
1 Force Technology Norway AS, Sandvika, Norway
2 University of Groningen, Groningen, The Netherlands
3 MARIN, Wageningen, The Netherlands

ABSTRACT

Sloshing dynamics in LNG tanks is studied by carrying out numerical simulations. The applied CFD code ComFLOW solves the Navier-Stokes equations and uses an improved Volume-of-Fluid (iVOF) method to track the movement of the free surface. Application of two different fluid models, single-phase (only liquid) and two-phase (liquid and a compressible gas) is presented, the latter model being capable of simulating bubbles of gas entrapped in liquid. For single-phase simulations the SOR method is applied to solve the pressure field, while the BiCGSTAB pressure solver is used in case of two-phase simulations.

In the future, numerical results will be verified against measured data from two-dimensional tank sections, which will be provided by Daewoo Shipbuilding and Marine Engineering. Currently all simulations are blind calculations, since experimental results are not yet available to the authors. The CFD results will be shown for tank filling rates of 20% and 70%, and will include both fluid heights in the tank and fluid pressures exerted on tank walls. Results are obtained on two grids and a visual inspection in the form of computer animation frames is included as well.

KEY WORDS: Sloshing, Numerical Simulation, Volume-of-Fluid Method, Two-Phase Flow.

INTRODUCTION

The sloshing motion of fluid inside partially-filled tanks receives growing attention during the last years. Especially with the trend towards tanks of membrane type, sloshing onboard LNG carriers has become an important topic of research. The fluid distribution in these tanks strongly depends on both tank filling ratio and ship motion.

Inside the tanks, the fluid is generally a complex mixture of different fluids, with increasing complexity for higher filling ratios and large motion amplitudes. The free surface motion is highly nonlinear with run-up against tank walls and frequent entrapment of gas bubbles. Taking into account the fluid properties of LNG makes the description of the sloshing flow even more complex.

The total impact load on the tank walls due to sloshing motion can be determined by integrating measured or computed pressure values along the tank walls. To estimate the total load accurately, the pressure should be measured on proper locations along the walls in order to catch short-lasting and localized pressure peaks. Effects of fluid-structure interaction on impact loads and ship response have been described recently in Kim (2007) and Jung (2008).

The nonlinearity of the free surface and frequent entrapment of gas bubbles make simulation of the sloshing flow very complex and generally beyond the limits of potential flow models. One of the methods applied to simulate sloshing flows is the Smooth Particle Hydrodynamics (SPH) method (Colagrossi 2007, Iglesias 2004, Nam 2006). Also the Level-Set (LS) method is used for sloshing problems (Yu 2007). A different approach to tackle the sloshing problem is the Volume-of-Fluid method. The advantage of using the Volume-of-Fluid method is its sharp description of the free surface, which is especially beneficial in case of strongly nonlinear motion of the free surface.

The numerical method described in this paper uses a local height function to improve the description of the free surface. By improving the Volume-Of-Fluid method in this way, mass losses due to numerical flaws are minimized (Kleefsman 2005).

Especially for cases with high tank filling ratios and corresponding irregular and nonlinear free surface motion it is beneficial to model the flow using both liquid and gas phases. This is not only because it improves the description of global fluid motion and damping effects, but also because entrapment and entrainment of gas bubbles occur frequently in these cases (Bunnik 2007). Recent comparisons of the two-phase flow model with experimental results have been reported in Wemmenhove (2008) and Iwanowski (2009).

This paper shows results of a sloshing study for a rectangular tank section and for a section with four chambers. Tank motion is regular sway in this study while two motion amplitudes and two tank filling ratios are considered. Attention will be paid to an accurate description of both fluid distribution and pressure levels.

THE COMFLOW PROGRAM

The 3D CFD solver ComFLOW has been developed by the University of Groningen, The Netherlands. The code has been continuously and actively developed within the Joint Industry Projects SAFE-FLOW (2001-2004) and ComFLOW-2 (2005-2008).

The ComFLOW program can employ one of two basic physical models

for sloshing calculations, either single-phase (only liquid) or two-phase (liquid and compressible gas). The latter model is recommended for sloshing calculations with higher tank filling ratios. A local height function is used as an improvement over the original VOF algorithm (Hirt 1981).

The theoretical model is based on one set of equations that describes the behaviour of two different fluids together. The continuity and momentum equations for the two-phase flow read:

$$\frac{\partial \rho}{\partial t} + \nabla \cdot (\rho u) = 0 \qquad (1)$$

$$\frac{\partial (\rho u)}{\partial t} + \nabla \cdot (\rho u u) + \nabla p$$
$$- \nabla \cdot \left(\mu (\nabla u + \nabla u^T) - \tfrac{2}{3} \mu \nabla \cdot u \right) - \rho F = 0 \qquad (2)$$

with $u = (u,v,w)$ being the fluid velocity vector, p its pressure, ρ its density, and μ its dynamic viscosity coefficient. Further, t denotes time and $F = (Fx,Fy,Fz)$ is an external body force, for example gravity. In case of two-phase flow the density ρ appears as a variable and it is necessary to close the system of equations by relating the pressure and density of the fluid. The pressure field is computed by solving the compressible form of the Poisson equation, see (Wemmenhove 2008). This equation includes an adiabatic equation of state for the compressible phase with a polytropic coefficient of $\gamma=1.4$:

$$\frac{p_{gas}}{p_{ref}} = \left(\frac{\rho_{gas}}{\rho_{ref}} \right)^{\gamma} \qquad (3)$$

In the liquid phase this relation is replaced by

$$\rho = \rho_{liq} \qquad (4)$$

Thus, (1) and (2) form a unified description for both phases; their only distinction being the choice for the equation of state: (3) or (4)

ALGORITHMIC CONSIDERATIONS

The following issues are of importance when simulating sloshing dynamics:

- Choice of grid and grid convergence
- Free surface reconstruction
- (Numerical) Damping of fluid motion
- Averaging of density and viscosity

GRID OPTIMIZATION

The numerical method employs a Cartesian grid with a cut-cell method at boundaries of the computational domain. More details about the cut-cell method can be found in (Kleefsman 2005).

If the computational results will be compared with experimental data, it is important to position fluid height probes and pressure control points carefully in the computational grid. ComFLOW employs a staggered grid, which means that fluid height probes and pressure control points should be positioned in cell centers for the best accuracy. Hence the grid has to be designed such that each pressure control point is positioned as close as possible to a cell center. Figure 1 shows an example where the grid is designed such that all pressure sensors are located in cell centers.
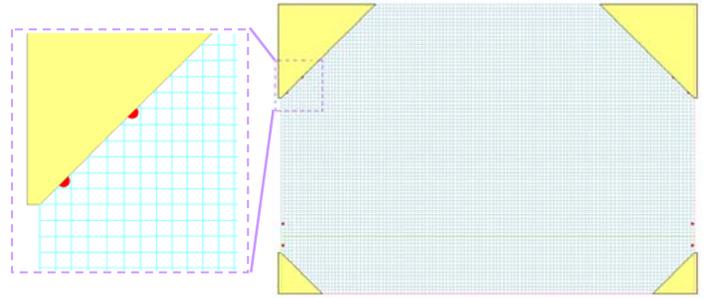

Figure 1 *Positioning of pressure transducers (red points) in transverse cross-section*

The total number of grid cells should be kept as low as possible to reduce computational times, although some minimum of cells is necessary. Obviously, this minimum can be subject of discussion and depends on the tank geometry. A reasonable grid resolution is required to catch the dynamics of bubbles, droplets, fluid tongues etc.

FREE SURFACE RECONSTRUCTION

The fluid inside a sloshing tank is subjected to body forces in vertical and horizontal directions due to gravity and ship motions. This results in a rather irregular fluid distribution, especially for higher tank filling ratios and large motion frequencies. As mentioned, such fluid configurations may consist of water tongues, droplets and entrapped gas bubbles. The free surface has to be reconstructed in a way that no additional unphysical droplets are created. A local height function is used to overcome problems of the traditional VOF algorithm with flotsam and jetsam, i.e. unphysical isolated droplets. The local height function considers a block of 3x3 (2D) or 3x3x3 (3D) cells around a free surface cell to determine the orientation of the free surface. More details can be found in (Kleefsman 2005).

For many sloshing cases it is beneficial to model the fluid dynamics of both liquid and gas phases. Although the active number of computational cells increases, modeling both phases gives a more complete picture of the overall fluid dynamics with a continuous velocity field across the free surface. Figure 2 shows entrapment of an air pocket during a low filling ratio sloshing experiment. In this case it is desirable to model both phases and include the compressible behaviour of the air pocket.
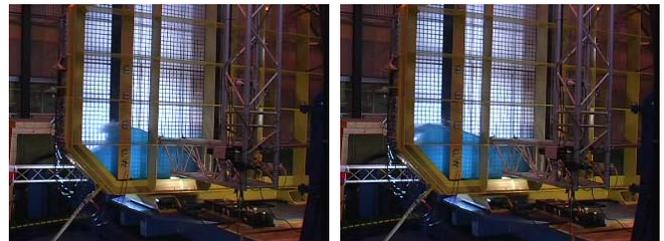

Figure 2 *Air entrapment during MARIN sloshing experiments*

Modeling of both phases means that the local height function can still be used to reconstruct the free surface. On the other hand, it requires use of appropriate numerical schemes and pressure solvers. It also introduces new sensitivities due to large variations in the density of the fluid (up to a factor of 1000) across the free surface. A careful discretisation of the density at the free surface is required to prevent irregularities in the velocity field (Wemmenhove 2008).

Figure 3 *Free surface for low filling ratio sloshing calculations with simple (left) and gravity-consistent (right) density averaging methods*

Figure 3 shows the free surface in a low filling ratio sloshing computation (corresponding to the experiment shown in Figure 2) with two density averaging methods, the cell-weighted averaging method and the gravity-consistent averaging method. Only the latter method ensures correct balance between pressure gradient and body force for hydrostatic conditions (Wemmenhove 2008). The discretely averaged density then satisfies $\nabla \times (\rho F) = 0$ in equilibrium.

CONVECTION

Given their magnitude within the Navier-Stokes equations, a proper discretisation of the convective terms is very important. The often used 1st order upwind differencing scheme, hereafter denoted as B2, introduces a large amount of artificial dissipation. Therefore, the 2nd order upwind differencing scheme (denoted as B3) has been used in order to limit the amount of numerical damping caused by the upwind differencing itself.

The 2nd order upwind scheme gives less numerical damping, but also requires a change in time integration algorithm. The forward Euler method involving two time levels of variables:

$$\phi^{n+1} = \phi^n + \Delta t\, f\!\left(\phi^n\right), \tag{5}$$

is suitable when B2 is used. However, three time levels of variables and Adams-Bashforth time integration are desirable in combination with B3

$$\phi^{n+1} = \phi^n + \Delta t\, f\!\left(\tfrac{3}{2}\phi^n - \tfrac{1}{2}\phi^{n-1}\right) \tag{6}$$

Table 1. CFL number limits η_{max} for different schemes

	B2 upwind	B3 upwind
Forward Euler	$1 - d \approx 1$	$\sqrt{d} \ll 1$
Adams-Bashforth	$0.5 - d \approx 0.5$	$0.25 - 0.5d \approx 0.25$

Table 1 shows the CFL number stability limits for four combinations of spatial (B2 and B3) and time integration (Forward Euler and Adams-Bashforth) schemes. In convection-dominated flows the CFL number η controls the stability, while the diffusive parameter d is usually small. Table 1 indicates that in case of B3, the Forward Euler stability limit becomes very stringent, $\eta < \sqrt{d} \ll 1$. In contrast, the Adams-Bashforth time integration scheme is much more suitable for the B3 scheme, although it leads to a CFL limit that is about four times lower than for the B2 scheme.

PRESSURE COMPUTATION

Computational times are substantial for the sloshing analyses due to a highly irregular flow and long simulation times involved, especially for fine grids. Major part of the computational effort is required for solving the pressure field. For single-phase calculations, Successive Over Relaxation (SOR) is used as pressure solver. For two-phase models the BiCGSTAB (Stabilized Bi-Conjugate Gradient Method) solver is applied as a robust pressure solver, since it better handles the matrix structure resulting from large density ratios at the free surface.

At first sight, the two-phase flow computations seem to take much longer time due to the increased number of active computational cells. However, this is only a clear drawback for low tank filling ratios. For high filling ratio cases there is a smaller increase in the number of active computational cells when both phases are modeled. Computational costs are not always significantly higher (and can be even lower) for these cases when modeling two-phase flow. Although efficiency of calculations is important, it has to be stressed that increased computational costs are easily justified when results are more accurate because of the use of a two-phase model.

REMOVAL OF PRESSURE SPIKES

Pressure spikes do occasionally appear in computed time-pressure signals, especially in grid cells where the free surface has just appeared or just vanished. These spikes are numerically induced and it is therefore justified to use a reasonably designed peak-removal and curve smoothing procedure. The applied peak-removal and/or smoothing technique should be rather delicate to avoid smoothing out the truly existing flow features. All time-pressure curves obtained from the ComFLOW simulations have been post-processed by a multi-pass peak-removal and smoothing procedure. The data processing stages included:

1. re-sampling
2. removal of standalone peaks (pressure peaks with a very short duration, like one CFD time step, are considered as non-physical)
3. median filter
4. moving average filter with a Gauss or Kaiser window

Figure 4 shows an example of the data processing method with pressure signals before and after the peak-removal and smoothing procedure. It can be seen that the original time-pressure signals (red colour curves) are somewhat shaky and that there are spikes. The post-processed curves are displayed in blue colour.
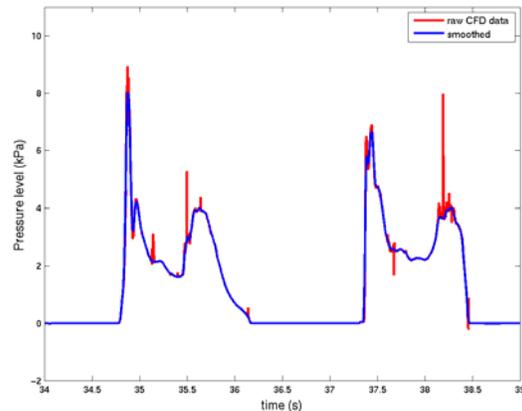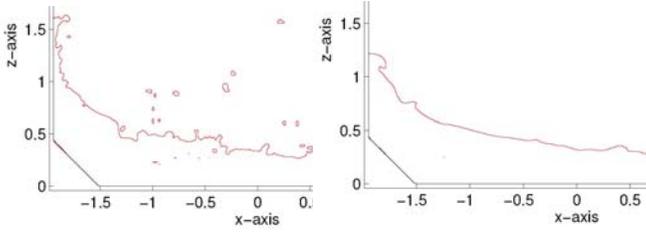

Figure 4 *Smoothing of pressure signal*

SLOSHING IN LONGITUDINAL TANK SECTION

Figure 5 shows the geometry of a longitudinal section of a membrane-type LNG tank. It includes locations of pressure sensors P1-P8 and fluid height probes WH1 and WH8.
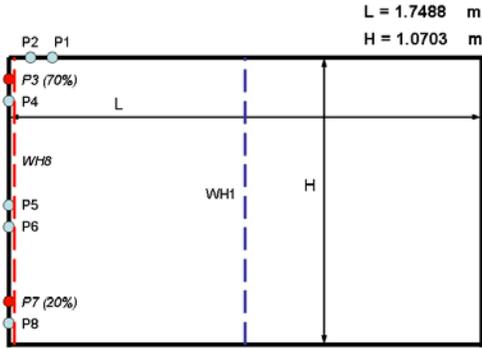

Figure 5 *Longitudinal tank geometry*

Both low-filling and high-filling ratio fluid configurations are of interest and have been studied for the longitudinal tank section. The motion of the tank is harmonic with amplitudes (small and large) and frequencies for four test cases listed in Table 2. The tank motion signal is multiplied by a half-cosine ramp function during the first three periods of simulation.

Table 2. Longitudinal tank test cases

Case Index	Description	Fill	Freq (Hz)	Ampl (m)
L-R2F1A1	20-LONG-SMALL	20%	0.4046	0.17488
L-R2F1A2	20-LONG-LARGE	20%	0.4046	0.34976
L-R7F2A1	70-LONG-SMALL	70%	0.6243	0.17488
L-R7F1A2	70-LONG-LARGE	70%	0.6243	0.34976

As discussed earlier, the grid is chosen such that computational times are within reasonable limits, while fluid height probes and pressure control points are positioned in cell centers. The following grids have been used for the longitudinal tank section calculations:

Table 3. Grids for longitudinal tank sectio*n*

Grid	Dgrid (m)	Cells	Total # cells
A	0.0133	131 x 1 x 81	10611
B	0.0080	219 x 1 x 133	29127
3D	0.0133	131 x 11 x 81	116721

The finest grid (B) in Table 3 consists of cells only marginally larger than the pressure transducers used in the experiments by Daewoo Shipbuilding and Marine Engineering. Therefore, this grid is chosen as the finest grid when studying grid convergence.

Fluid distribution has been inspected visually by means of 2D and 3D animations. Figure 6 shows two typical fluid configurations (3D animations) for the large amplitude 20% filling ratio test. The run-up against the tank wall in the left picture is quickly followed by the bore motion with hydraulic jump in the right picture.

Fluid distribution and pressure values should be similar for 2D and 3D simulations, since there is no real tank motion component in the third direction. Water heights and pressure signals are reported for 2D simulations, as 3D animations only show small differences in fluid distributions in the third direction across the tank thickness.
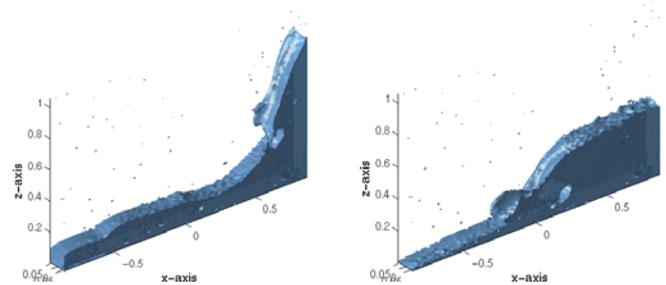

Figure 6 *Fluid configuration for test 20-LONG-LARGE with 3D grid, t = 36.5s (left) and t=37.0s (right).*
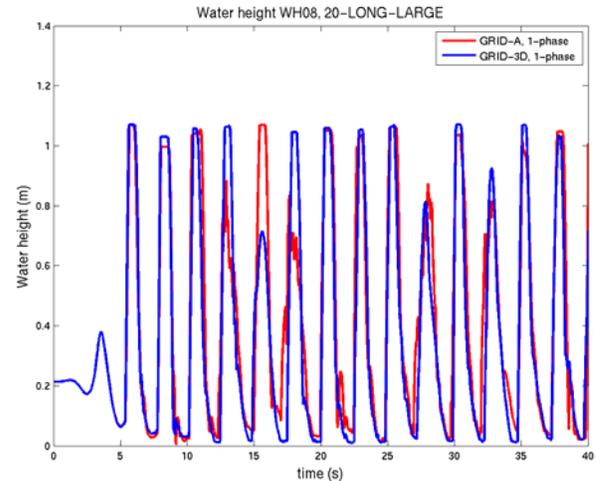

Figure 7 *Fluid run-up at fluid height probe WH08 (left tank wall) for test 20-LONG-LARGE with 2D and 3D grid.*

Figure 7 shows an example where 2D and 3D simulations give comparable levels of run-up.

Water heights have been recorded at the tank center and also at eight other locations, including side walls of the tank section to estimate run-up. Water heights are reported at fluid height probe WH08 immediately near the left wall in Figure 8, since pressures are recorded along this wall as well. Note that the fluid height probe is completely wet during most of each sloshing period in the high filling ratio cases. Computational pressures have been recorded at 4 (20% filling) or 6 (70% filling) locations. Pressure signals are displayed in Figure 9 for transducer P07 for 20% filling and for transducer P03 in case of 70% filling. Water heights and pressures are shown for 4-6 sloshing periods to improve legibility of the figures.

The 20% filling ratio cases have been computed with use of the one-phase flow model. The pressure signal in transducer P07 is rather repetitive (although pressure spikes occur) with maximum values up to 6-8 kPa for the low amplitude case and up to 14 kPa for the high-amplitude case.

For the 70% filling ratio cases the fluid flow is much more irregular with frequent occurrence of air entrapment and water tongues. Due to the complex flow, results for 70% filling ratio have been acquired by computing two-phase flow. Pressure transducer P03 is located near the top corner of the tank section, a location where the free surface passes frequently. This leads to a relatively shaky pressure signal. Maximum pressure levels are estimated at about 12 kPa for the small motion amplitude case and up to 18 kPa for the large motion amplitude case.
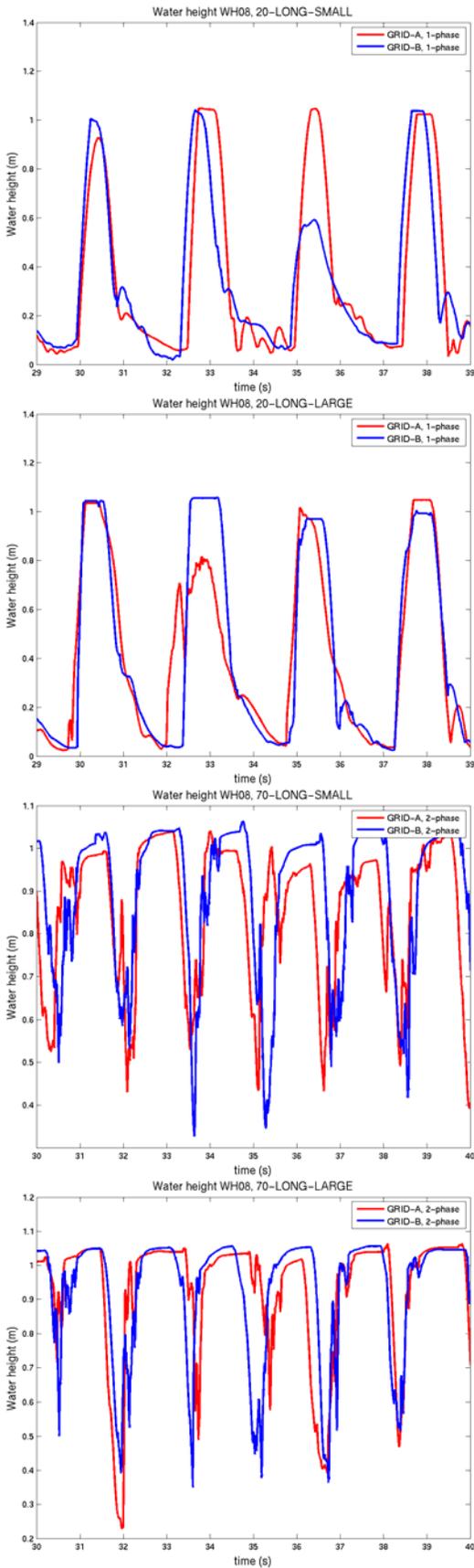
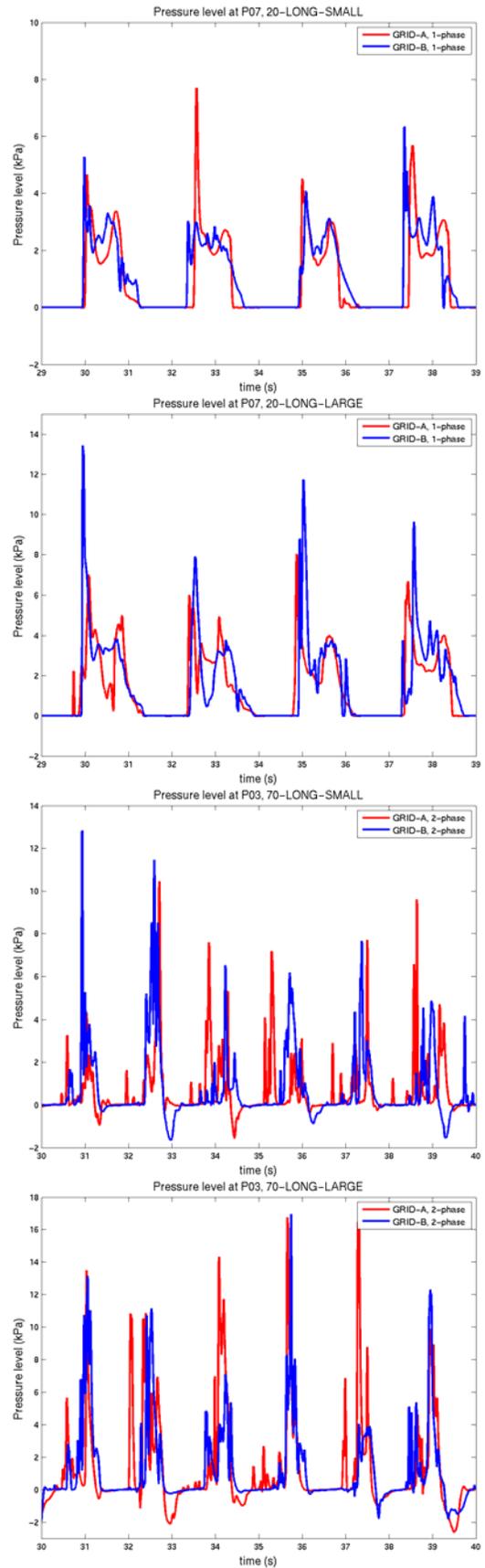Figure 8 *Water height at left side wall of longitudinal tank section*

Figure 9 *Filtered pressure signals for longitudinal tank section*

SLOSHING IN TRANSVERSE TANK SECTION

Figure 10 shows the geometry of a transverse section of a membrane-type LNG tank. Four cases of motion amplitude and filling ratio have been studied for the transverse tank section and are listed in Table 4.
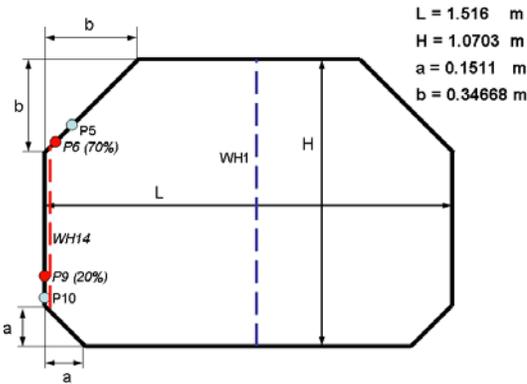

Figure 10 *Transverse tank geometry*

Compared to the slightly longer longitudinal tank section, the excitation periods are now shorter and motion amplitudes are smaller. Again, the tank motion signal is multiplied by a half-cosine ramp function during the first three periods of simulation.

Table 4.   Transverse test cases

Case Index	Description	Fill	Freq (Hz)	Ampl (m)
T-R2F2A1	20-TRAN-SMALL	20%	0.4632	0.1516
T-R2F2A2	20-TRAN-LARGE	20%	0.4632	0.3032
T-R7F2A1	70-TRAN-SMALL	70%	0.6861	0.1516
T-R7F2A2	70-TRAN-LARGE	70%	0.6861	0.3032

The grid is designed such that fluid height probes and pressure control points, also those near the chambers in the corners of the cross-section, are positioned in cell centers. The following grids have been used for the transverse tank section calculations:

Table 5.   Grids for transverse tank section

Grid	Dgrid (m)	Cells	Total # cells
A	0.0132	115 x 1 x 81	9315
B	0.0079	191 x 1 x 135	25785
3D	0.0132	115 x 11 x 81	102465

Fluid height probes are positioned at various locations in the tank section. Before analyzing and evaluating pressure levels at the tank walls, it is insightful to verify the fluid distribution and in particular run-up motion of the fluid against side walls.

Figure 11 shows the run-up of the fluid against the left (WH14) tank wall in case of a transverse tank geometry with 20% filling ratio and large motion amplitude. After start-up there appears to be a rather regular run-up motion at the tank wall. The magnitudes of the run-up height do not seem to be perfectly consistent, especially the flat parts of the curves are not exactly at the same level. The recorded water heights are actually computed as the length of the wet part of a fluid height probe and are therefore by necessity sensitive to air bubbles or a water-air foam that could be present along the probe.

The fluid distribution has been inspected visually by means of 2D and 3D animations.

Figure 12 shows typical fluid configurations for both 20% and 70% filling ratio tests with small motion amplitude. Figure 13 shows the water height at the left wall of the transverse tank section for both filling ratios and both motion amplitudes.
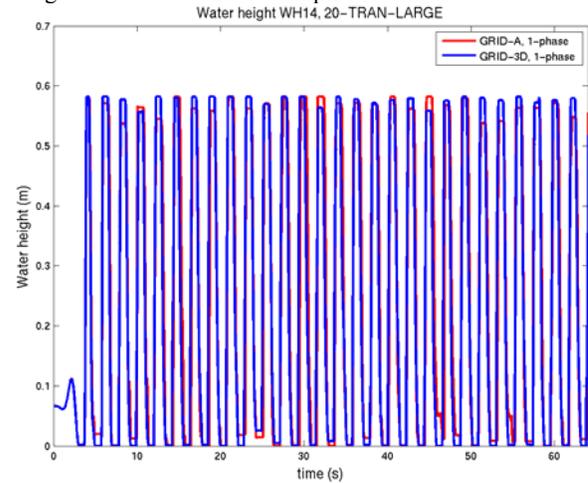

Figure 11 *Fluid run-up at fluid height probe WH14 (left tank wall) for test 20-TRAN-LARGE with 2D and 3D grid.*
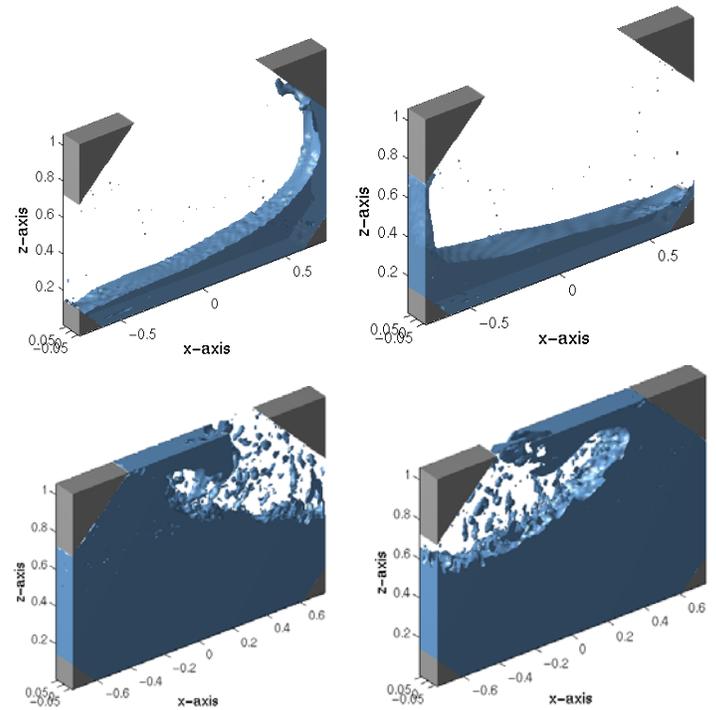

Figure 12 *Fluid configurations for tests 20-TRAN-SMALL (t=13.5s and t=14.5s) and 70-TRAN-SMALL (t=11.7s and t=12.3s) with 3D grid.*

The pressure signals at transducers P09 and P06 (see Figure 10), for low and high filling ratios respectively, are given in Figure 14. The 20% filling ratio cases have been computed by means of the SOR pressure solver, since the one-phase flow model is used. The pressure signal at transducer P09, near the lower chamber, shows peak pressures in the range of 4-5 kPa for the low amplitude case and up to 7 kPa for the high amplitude case.

Results for the 70% filling ratio cases have been obtained with the simulation of two-phase flow. Given the occurrence of typical two-phase flow phenomena such as air entrapment, this leads to a more accurate computation of fluid distribution and pressure field. The pressure signal at transducer P06, near the upper chamber, is displayed for 6 sloshing periods in Figure 14. Peak pressure values are estimated at 10-12 kPa for the small motion amplitude case and up to 16-18 kPa
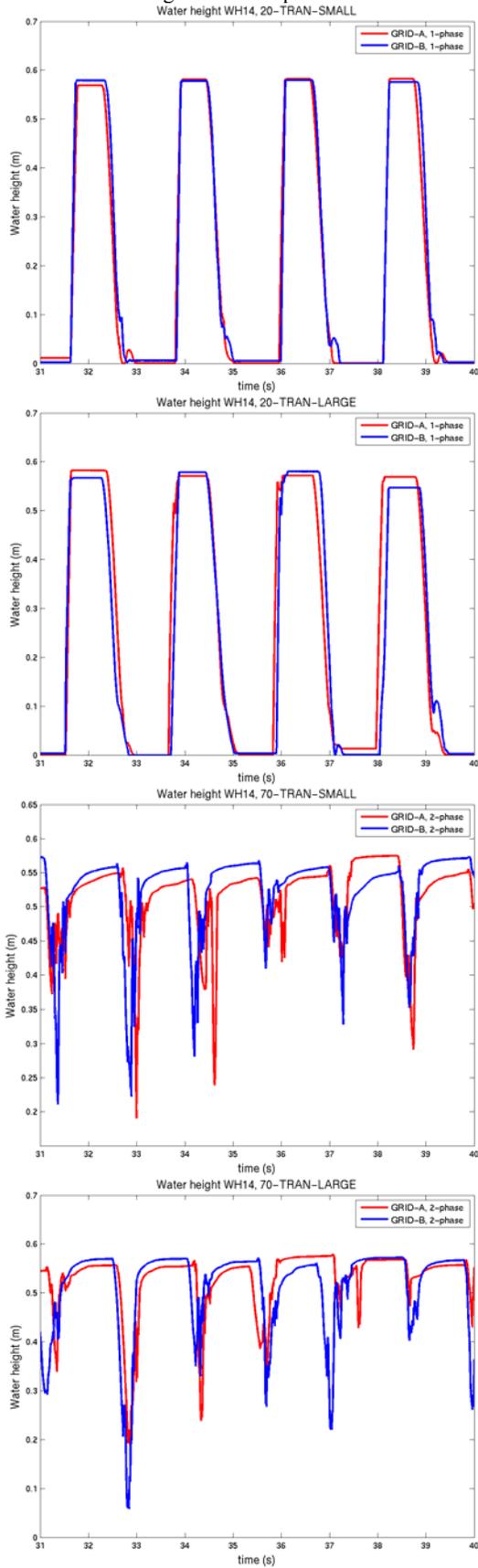
for the case of a large motion amplitude.

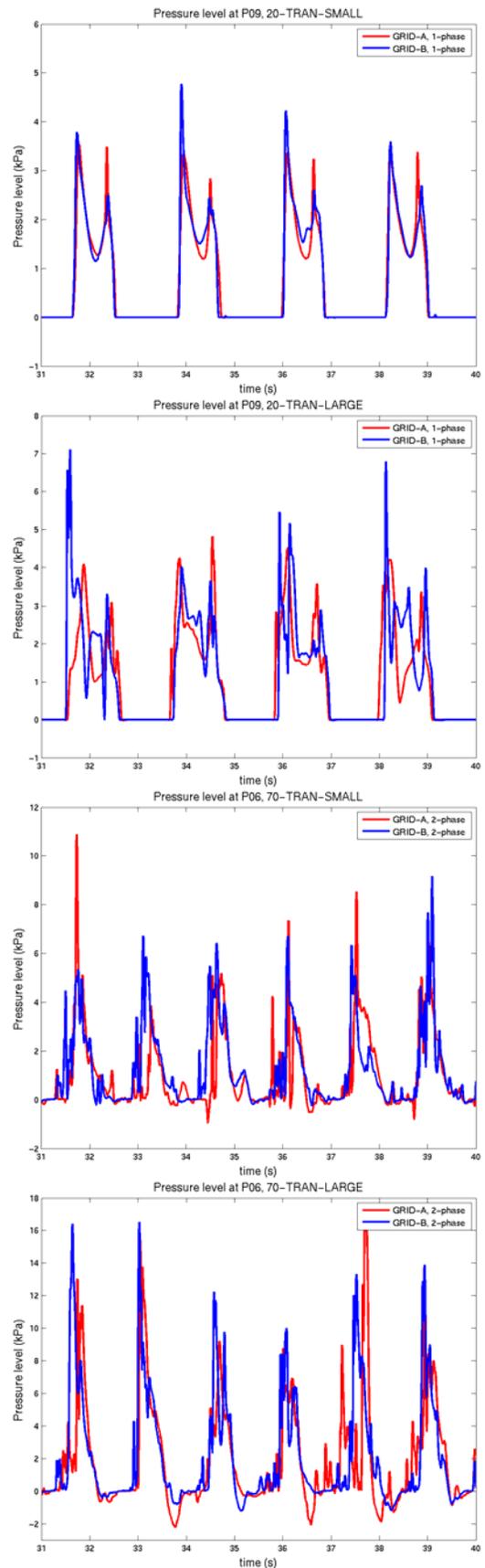Figure 13 *Water height at left wall of transverse tank*

Figure 14 *Filtered pressure signals for transverse tank section*

237

CONCLUSIONS

The ComFLOW program has been used to simulate sloshing for various filling ratios, tank cross-sections and motion amplitudes. Different grid resolutions have been examined and fluid distributions and pressure levels have been investigated. For all sloshing cases, a relatively fine grid is necessary to obtain sufficient grid convergence. Results of the examined grid resolutions agree fairly well, while further grid refinement would lead to excessive computational times.

The fluid flow is more complex for the higher 70% filling ratio cases than for the 20% filling ratio cases. In case of a low filling ratio it is sufficient to model only the flow in the liquid phase. The case of a high filling ratio of 70% is more demanding for numerical simulation due to the more complex flow features. For this case a more accurate and efficient alternative is to simulate two-phase flow.

To prevent numerically-induced pressure spikes, a peak-removal and smoothing technique has been applied. This method does not smooth out the truly existing flow features, but rather cuts away pressure spikes and thereby improves the legibility of pressure signals. As expected, peak pressure values increase for increasing tank filling ratio and higher tank motion amplitudes. Final conclusions will be drawn by validation of these pressure values with experimental results to be provided by Daewoo Shipbuilding and Marine Engineering.

REFERENCES

Bunnik, Tim and Huijsmans, Rene. *"Large scale LNG Sloshing Model Tests,"* 17th (2007) Int Offshore and Polar Eng Conf, Lisbon, Portugal, ISOPE, pp 1893–1899.

Colagrossi, A. and Colicchio, G. *"Investigation of some naval hydrodynamics problems through a SPH methods,"* Computational Methods in Marine Engineering II (2007), Barcelona, Spain.

Hirt, C.W. and Nichols, B.D. (1981). "*Volume Of Fluid (VOF) Method for the Dynamics of Free Boundaries,*" *Journal of Computational Physics*, Vol 39, pp 201-225.

Iglesias, A.S., Rojas, L.P. and Rodriguez, R.Z. (2004). "*Simulation of anti-roll tanks and sloshing type problems with smoothed particle hydrodynamics,*" *Ocean Engineering*, Vol 31, pp 1169-1192.

Iwanowski, B., Lefranc, M. and Wemmenhove, R. *"Numerical simulation of sloshing in a tank, CFD calculations against model tests,"* 28th (2009) Int Conf on Offshore Mech and Arctic Eng, Honolulu, USA, paper OMAE2009-79051, submitted.

Jung, J., Lee, H., Park, T. and Lee, Y. *"Experimental and numerical investigation into the effects of fluid-structure interaction on the sloshing impact loads in membrane LNG carriers,"* 27th (2008) Int Conf on Offshore Mech and Arctic Eng, Estoril, Portugal, paper 2008-57323.

Kim, J.W. and Kim, K. *"Response-based evaluation of design sloshing loads for membrane-type LNG carriers,"* 26th (2007) Int Conf on Offshore Mech and Arctic Eng, San Diego, USA, paper 2007-29746.

Kleefsman, K.M.T., Fekken, G., Veldman, A.E.P., Buchner, B., Iwanowski, B (2005). *"A Volume-Of-Fluid Based Simulation Method For Wave Impact Problems,"* Journal of Computational Physics, Vol 31, pp 363-393

Nam, Bo-Woo and Kim, Yongwhan. *"Simulation of Two-Dimensional Sloshing Flows by SPH Method,"* 16th (2006) Int Offshore and Polar Eng Conf, San Francisco, USA.

Wemmenhove, R., Luppes, R., Veldman, A.E.P. and Bunnik, T. *"Application of a VOF method to model compressible two-phase flow in sloshing tanks,"* 27th (2008) Int Conf on Offshore Mech and Arctic Eng, Estoril, Portugal, paper 2008-57254.

Wemmenhove, R. (2008). "Numerical simulation of two-phase flow in offshore environments," PhD Thesis, University of Groningen, The Netherlands.

Yu, K. Chen, H.C., Kim, J.W. and Lee, Y.B. *"Numerical simulation of two-phase sloshing flow in LNG tank using finite-analytic level-set method ,"* 26th (2007) Int Conf on Offshore Mech and Arctic Eng, San Diego, USA, paper 2007-29745.